Computing Highly Accurate GW Waveforms for Extreme Mass Ratio Inspirals

JONATHAN THORNBURG[1] AND BARRY WARDELL[2]

[1] Astronomy Department & Center for Spacetime Symmetries, Indiana University, Bloomington, Indiana, USA
[2] Max-Planck-Institut für Gravitationsphysik, Albert-Einstein-Institut, Golm, Germany

Introduction

An extreme mass ratio inspiral (EMRI) system is a binary BH system with an extreme mass ratio $\mu := M_1/M_2 \ll 1$. A typical EMRI ($\sim 10 : 10^6 M_\odot$) accumulates $\sim 10^6$ radians of GW phase in the last year before merger, so phase-coherent modelling and matched filtering of the GW waveform allows very precise strong-field GR tests. To do this, and indeed even to detect weak EMRI signals in the presence of stronger signals, we need to model the GW phase to high accuracy, preferably $\lesssim 1/\rho$ radians over the entire inspiral, where ρ is the signal/noise ratio of the EMRI signal after matched filtering. That is, we need to model the instantaneous orbital frequency to $\lesssim 1/\rho$ parts per million (ppm) accuracy.

While EMRI GWs are much weaker than those from a comparable-mass supermassive BH inspiral, EMRI inspirals last for *much* longer: the rate of orbital evolution scales with the mass ratio $\mu \sim 10^{-5}$, so the system makes $\mathcal{O}(\mu^{-1}) \sim 10^5$ orbits in the strong-field region. LISA (if funded) should see many such systems at redshifts out to $z \sim 1$, with nearby systems having $\rho \gtrsim 100$. The orbit will typically remain quite eccentric through merger. EMRI GW waveforms are very complicated, with multiple quasi-periodicities encoding various parts of the orbital dynamics (figure 1).
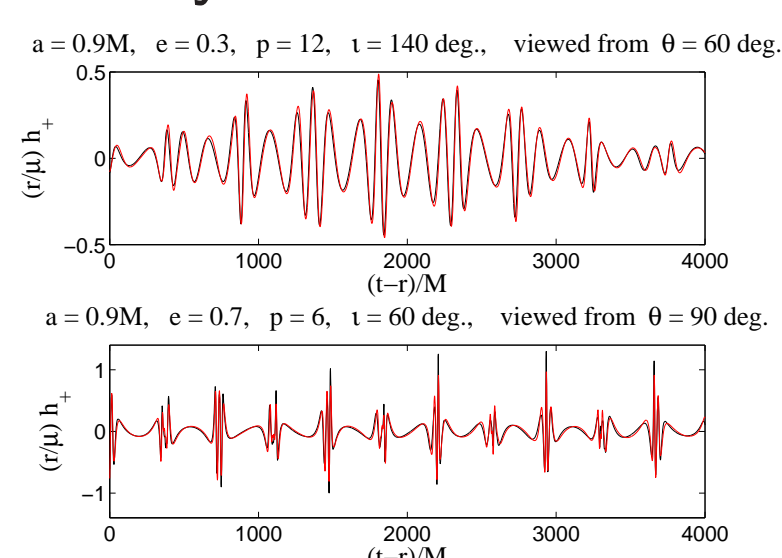
Figure 1: Approximate EMRI waveforms (figure adapted from S. Drasco, *CQG* **23**, S769).

Because of the very long time span and very high accuracy requirements, it's not practical to compute EMRI GWs by direct numerical integration of the Einstein equations. Instead, BH perturbation theory is used, modelling the EMRI system as the large BH's "background" (Schwarzschild/Kerr) spacetime together with an $\mathcal{O}(\mu)$ perturbation due to the small BH. For general surveys of this research program, see [5, 9].

As a step towards highly accurate EMRI GW templates, here we consider the problem of calculating the radiation-reaction "self-force" on the small body ("particle") to very high accuracy, for the model system of a scalar-field particle in an arbitrary bound geodesic orbit in Schwarzschild or Kerr spacetime. We discuss two methods for this: the Barack-Ori "mode-sum regularization" method (work by JT) and the Barack-Golbourn-Vega-Detweiler "effective source" method (work by JT & BW).

For both methods, it's convenient to model the small BH as a point particle. The scalar field Φ due to the particle satisfies

$$\Box\Phi = -4\pi q \int_{-\infty}^{+\infty} \frac{\delta(x^a - x^a_{\text{particle}}(\tau'))}{\sqrt{-g}}\,d\tau' \qquad (1)$$

where q is the particle's scalar charge, and the integration is over the particle's entire worldline. Unfortunately, for a point particle Φ is formally infinite at the particle, so we can't numerically solve (1) or compute the self-force $F^a = q(\nabla^a\Phi)\big|_{\text{particle}}$.

Mode-Sum Regularization

The Barack-Ori mode-sum regularization [2] is derived from a formal Green-function solution to (1), followed by a spherical-harmonic decomposition of the scalar field,

$$\Phi(t, r, \theta, \phi) = \sum_{\ell=0}^{\infty} \sum_{m=-\ell}^{\ell} Y_{\ell m}(\theta, \phi)\varphi_{\ell m}(t, r) \qquad (2)$$

For motion in Schwarzschild spacetime, each individual spherical-harmonic mode then satisfies a linear complex wave equation in 1+1 D on the Schwarzschild background,

$$\Box\varphi_{\ell m} + V_\ell(r)\varphi_{\ell m} = S_{\ell m}(t)\delta(r - r_{\text{particle}}(t)) \qquad (3)$$

where the potential $V_\ell(r)$ and source amplitude $S_{\ell m}(t)$ are known analytically. For Kerr spacetime a similar result holds, although the different ℓm modes are coupled [3].

Numerically Computing the Fields $\varphi_{\ell m}$

I (JT) numerically solve (3) for each ℓm using double-null (characteristic) coordinates/grids, using a variant of the usual Berger-Oliger AMR algorithm adapted for characteristic grids [8]. (This AMR code is freely available to other researchers; see the arXiv paper.) I obtain excellent 4th order convergence, even near the particle where $\varphi_{\ell m}$ is non-differentiable (figure 2).
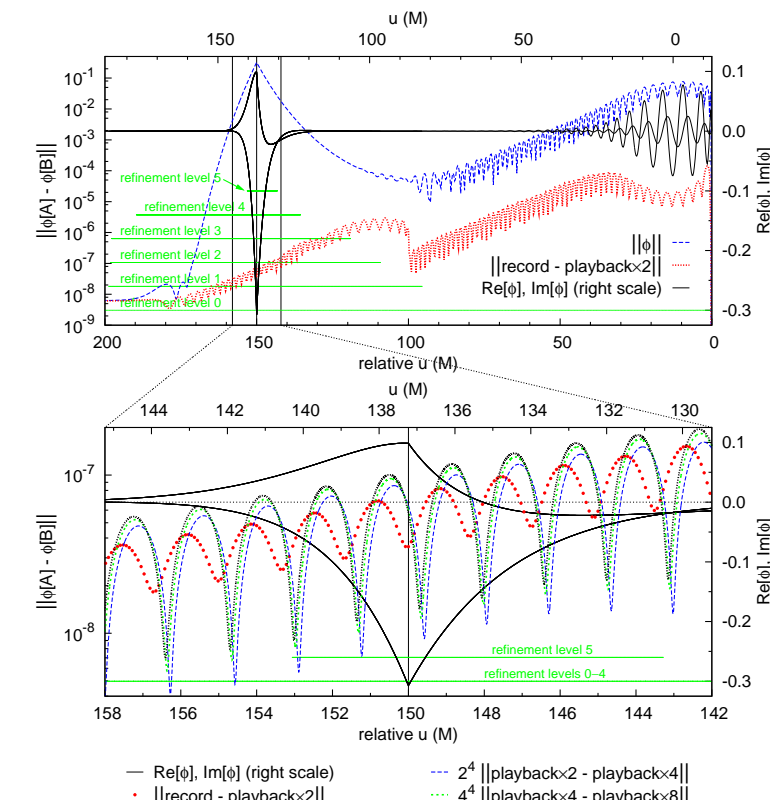
Figure 2: 4th order convergence of the characteristic AMR algorithm with grid resolution.

Boundary Conditions and Problem Domain

The true (physical) boundary conditions for (3) are only specified at $\mathcal{J}^\pm$. I numerically solve (3) on a finite double-null "diamond" domain using arbitrary (null) initial data (figure 3). The initial data generates a burst of spurious radiation, but this propagates away and $\varphi_{\ell m}$ eventually settles down to an equilibrium state, allowing the self-force to be calculated at the "top" of the numerical domain (figure 3). My numerical results show no evidence of persistent Jost junk solutions [6].

The time required to reach this equilibrium state (to within some specified numerical error tolerance) – and thus the required size of the double-null numerical problem domain – varies strongly with ℓ. For very high accuracy I have used problem domains up to $(100\,000M)^2$ for $\ell = 0$, decreasing to $(400M)^2$ for $\ell \geq 5$.
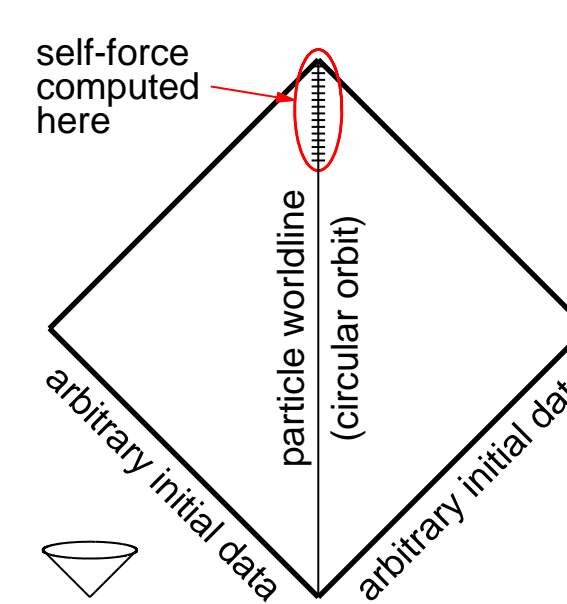
Figure 3: Double-null "diamond" problem domain for characteristic evolution.

Computing the Self-Force

The self-force on the particle is given by

$$F^a = \sum_{\ell=0}^{\infty} \left(F^a_{\ell\pm} - \left[\pm A^a(\ell + \tfrac{1}{2}) + B^a + C^a(\ell + \tfrac{1}{2})^{-1}\right] \right) \qquad (4)$$

where A^a, B^a, and C^a are analytically calculable, and $F^a_{\ell\pm}$ can be computed from $\sum_m \nabla\varphi_{\ell m}$ at the particle, taking 1-sided derivatives of $\varphi_{\ell m}$ (which is non-differentiable there) from either outside ($+$) or inside ($-$) the particle position. (4) is an infinite sum; in practice I only compute $\varphi_{\ell m}$ up to $\ell \sim 30$. I then least-squares fit a large-ℓ asymptotic series to the numerically-computed $F^a_{\ell\pm}$, and use the fit coefficients to estimate the remainder of the infinite sum (4).

The numerical solution of (3) is quite delicate, and there are also serious cancellations in the sum (4). Double-precision floating-point rounding errors in solving (3) thus affect F^a_ℓ at the ~ 0.1 ppm level (figure 4), Using long-double (80-bit) floating-point arithmetic to solve (3), I [7] have obtained the self-force F^a to within $\lesssim 1$ ppm, as measured both by my internal error estimates and by comparison to highly-accurate frequency-domain results [4].
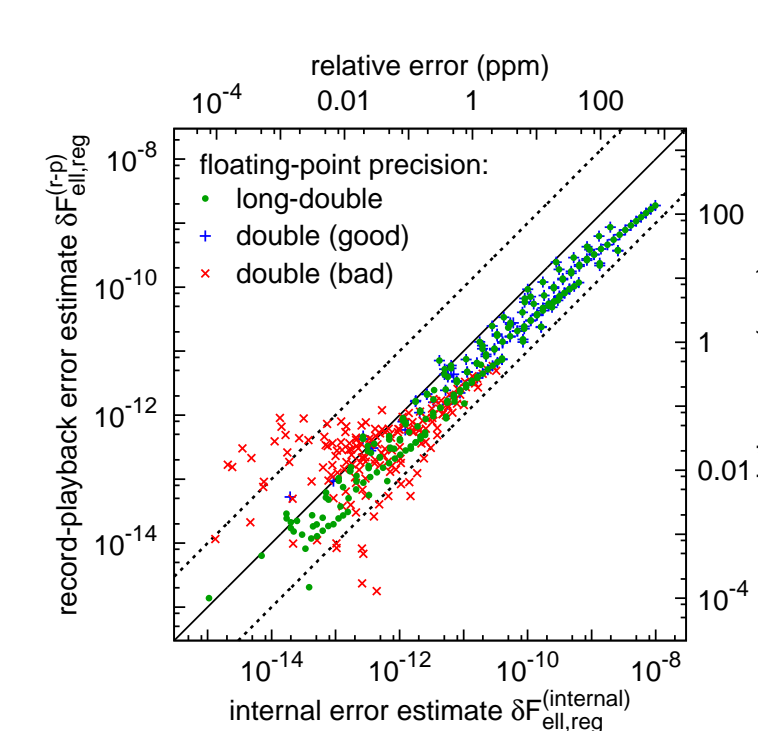
Figure 4: Scatterplot of F^a_ℓ actual ("record-playback") versus estimated ("internal") errors.

The Effective-Source Approach

Another way of computing the self-force is the effective-source method [1, 10]. Here we define a "puncture function" Φ_{punct} which approximates Φ near the particle, so that the "residual field" $\Phi_{\text{res}} := \Phi - \Phi_{\text{punct}}$ satisfies

$$\Box\Phi_{\text{res}} = S^{(3)}_{\text{eff}} \qquad (5)$$

where the "effective source" $S^{(3)}_{\text{eff}}$ is given by

$$S^{(3)}_{\text{eff}} = -\Box\Phi_{\text{punct}} - 4\pi q \int_{-\infty}^{\infty} \frac{\delta(x^a - x^a_{\text{particle}}(\tau'))}{\sqrt{-g}}\,d\tau' \qquad (6)$$

If Φ_{punct} is a sufficiently good approximation to Φ near the particle, then Φ_{res} and $S^{(3)}_{\text{eff}}$ are finite at the particle, (5) can be solved numerically, and $F^a = q(\nabla^a\Phi_{\text{res}})\big|_{\text{particle}}$.

The m-mode Decomposition

Rather than solving (5) numerically in 3+1 D, we (JT & BW) Fourier-decompose in the azimuthal (ϕ) direction,

$$\Phi(t, r, \theta, \phi) = \sum_{m=-\infty}^{\infty} e^{im\tilde\phi}\varphi_m(t, r_*, \theta) \qquad (7a)$$

$$S^{(3)}_{\text{eff}} = \sum_{m=-\infty}^{\infty} e^{im\tilde\phi}S^{(2)}_{\text{eff},m}(t, r_*, \theta) \qquad (7b)$$

where (t, r, θ, ϕ) are the usual Boyer-Lindquist coordinates in Kerr spacetime, $r_*(r)$ is a "tortise" radial coordinate, and $\tilde\phi := \phi + f(r)$ is an "untwisted" azimuthal coordinate chosen so as to be regular at the horizon. The individual Fourier modes $\varphi_{\text{res},m}$ now satisfy

$$\Box_m\varphi_{\text{res},m} = S^{(2)}_{\text{eff},m} \qquad (8)$$

where the "2-D puncture function" $\varphi_{\text{punct},m}$ and "2-D effective source" $S^{(2)}_{\text{eff},m}$ are given by

$$\varphi_{\text{punct},m} = \frac{1}{2\pi}\int_{-\pi}^{\pi}\Phi_{\text{punct}}(t, r, \theta, \phi)e^{-im\tilde\phi}\,d\tilde\phi \qquad (9a)$$

$$S^{(2)}_{\text{eff},m} = \frac{1}{2\pi}\int_{-\pi}^{\pi}S^{(3)}_{\text{eff}}(t, r, \theta, \phi)e^{-im\tilde\phi}\,d\tilde\phi \qquad (9b)$$

The Worldtube

Φ_{punct} and $S^{(3)}_{\text{eff}}$ can be computed near the particle using covariant Green-function expansions [12, 11]. Far from the particle these series diverge, so Φ_{punct} and $S^{(3)}_{\text{eff}}$ aren't defined. We thus define a worldtube surrounding the particle worldline in (r, θ) space, and replace (8) with

$$\Box_m\varphi_{\text{num},m} = \begin{cases} S^{(2)}_{\text{eff},m}, & \text{inside the worldtube} \\ 0 & \text{outside the worldtube} \end{cases} \qquad (10a)$$

where the "numerical field" $\varphi_{\text{num},m}$ satisfies the jump condition

$$(\varphi_{\text{num},m})_{\text{inside}} = (\varphi_{\text{num},m})_{\text{outside}} - \varphi_{\text{punct},m} \qquad (10b)$$

on the worldtube boundary. $S^{(2)}_{\text{eff},m}$ is needed only inside the worldtube, and $\varphi_{\text{punct},m}$ is needed only "near" (within a molecule-radius of) the worldtube boundary.

Computing the Puncture Function and Effective Source

A variety of different definitions are possible for Φ_{punct} and $S^{(3)}_{\text{eff}}$, with corresponding tradeoffs between the difficulty of computing them and the accuracy with which Φ_{punct} approximates the actual (singular) Φ near the particle. Here we use a "4th order" puncture, where $|\Phi_{\text{punct}} - \Phi| = \mathcal{O}(|\lambda|^3)$ near the particle, where λ is (roughly) the geodesic distance from the particle. Such a Φ_{punct} can be calculated as

$$\Phi_{\text{punct}}(\delta r, \delta\theta, \delta\phi) = \frac{\sum_{ijk} N_{ijk}(\delta r)^i(\delta\theta)^j(\delta\phi)^{(k)}}{\sum_{ijk} D_{ijk}(\delta r)^i(\delta\theta)^j(\delta\phi)^{(k)}} \qquad (11)$$

where there are 18 ijk terms in each sum, $(\delta r, \delta\theta, \delta\phi)$ is the coordinate position relative to the particle, $(\delta\phi)^{(k)}$ is a periodic function which approximates $(\delta\phi)^k$ near the particle, and the coefficients N_{ijk} and D_{ijk} are obtained via covariant Green-function expansions as lengthy but analytically-known functions of the particle position and velocity.

The Fourier integrals (9) can't be done analytically, so they must be computed numerically at (in general) each time step, for each $(\delta r, \delta\theta)$ grid point in the worldtube. To efficiently evaluate these integrals, at each time step we first compute the coefficients N_{ijk} and D_{ijk}, then compute the net coefficients of $(\delta\phi)^{(k)}$ in (11) at each $(\delta r, \delta\theta)$ grid point in or near the worldtube, then finally evaluate the integrals at each such grid point using a numerical quadrature routine (`gsl_integration_qawo` from the GSL) specifically designed for computing oscillatory integrals of the form $\int f(x)e^{ikx}\,dx$.

Numerically Computing the Fields $\varphi_{\text{num},m}$

We are currently constructing a numerical code to compute the fields $\varphi_{\text{num},m}$ using a 2+1 D AMR Cauchy evolution in (r_*, θ) space. The same boundary-conditions issue arises as with the mode-sum scheme; we use a Cauchy problem domain large enough that reflections from the timelike inner/outer boundaries don't reach the worldtube within the numerical evolution time.

Conclusions

Both the mode-sum and effective-source schemes allow accurate self-force computations. The effective-source scheme appears to avoid many of the cancellations in the mode-sum scheme and so should have a higher ratio of accuracy-of-self-force to accuracy-of-PDE-solution.

By allowing the numerical accuracy and problem-domain size to vary with m, the m-mode decomposition variant of the effective-source scheme should be more efficient and accurate than directly solving for Φ_{res} in 3+1 D. We hope to reach the $\lesssim 1$ ppm accuracy level within the next year.

References

[1] Leor Barack and Darren A. Golbourn. Scalar-field perturbations from a particle orbiting a black hole using numerical evolution in 2+1 dimensions. *Phys. Rev. D*, 76(4):044020, Aug 2007, arXiv:0705.3620.

[2] Leor Barack and Amos Ori. Mode sum regularization approach for the self-force in black hole spacetime. *Phys. Rev. D*, 61(6):061502(R), Feb 2000, gr-qc/9912010.

[3] Leor Barack and Amos Ori. Gravitational self-force on a particle orbiting a Kerr black hole. *Phys. Rev. Lett.*, 90(11):111101, Mar 2003, gr-qc/0212103.

[4] Steven Detweiler, Eirini Messaritaki, and Bernard F. Whiting. Self-force of a scalar field for circular orbits about a Schwarzschild black hole. *Phys. Rev. D*, 67(10):104016, May 2003, gr-qc/0205079.

[5] Steve Drasco. Strategies for observing extreme mass ratio inspirals. *Class. Quant. Grav.*, 23(19):S769–S784, Oct 2006, gr-qc/0604115.

[6] Scott E. Field, Jan S. Hesthaven, and Stephen R. Lau. Persistent junk solutions in time-domain modeling of extreme mass ratio binaries. *Phys. Rev. D*, 81(12):124030, Jun 2010, arXiv:1001.2578.

[7] Jonathan Thornburg. Highly accurate and efficient self-force computation using time-domain methods: Error estimates, validation, and optimization, 2010, arXiv:1006.3788.

[8] Jonathan Thornburg. Adaptive mesh refinement for characteristic grids. *General Relativity and Gravitation*, 43(5):1211–1251, 2011, arXiv:0909.0036.

[9] Jonathan Thornburg. The Capra research program for modelling extreme mass ratio inspirals. *GW Notes*, 5:3–53, Sep 2010 – Jan 2011 2011, arXiv:1102.2857.

[10] Ian Vega and Steven Detweiler. Regularization of fields for self-force problems in curved spacetime: Foundations and a time-domain application. *Phys. Rev. D*, 77(8):084008, Apr 2008, arXiv:0712.4405.

[11] Ian Vega, Barry Wardell, and Peter Diener. Effective source approach to self-force calculation, 2011, arXiv:1101.2925.

[12] Barry Wardell. *Green Functions and Radiation Reaction From a Spacetime Perspective*. PhD thesis, University College Dublin, Dublin, 2009, arXiv:0910.2634.